JOURNAL OF GUIDANCE, CONTROL, AND DYNAMICS
Vol. 36, No. 3, May–June 2013

Intercept Angle Missile Guidance Under Time Varying Acceleration Bounds

Ilan Taub*
Israel Aerospace Industries, Ben-Gurion International Airport, 70100 Lod, Israel
and
Tal Shima†
Technion — Israel Institute of Technology, 32000 Haifa, Israel

DOI: 10.2514/1.59139

A linear quadratic guidance law for a missile with a time varying acceleration constraint is presented. By introducing the constraint into the running cost, the optimization produces time varying gains that shape the missile's trajectory for avoiding no-capture zones. The guidance law is derived for a missile with high-order autopilot dynamics and a terminal intercept angle constraint against a maneuvering target. The acceleration constraint of aerodynamic steering missiles is usually trajectory dependent rather than time dependent. Transforming the constraint into a time-dependent function by analytical means might not be possible, due to the nonlinear nature of the constraint. The problem is alleviated using a simple iterative calculation. For practical implementation reasons, and in order to improve the guidance performance under model uncertainties and disturbances, the guidance command is decomposed into two separate optimizations: one for the acceleration constraint, for which the guidance gains are calculated by a predicted time to go, and the other for the autopilot dynamics, for which the gains are obtained by a real-time time-to-go calculation, resulting in a suboptimal guidance law. The performance of the proposed law is investigated using nonlinear planar simulation, for a missile with first-order autopilot dynamics.

Nomenclature

$\mathbf{A}$, $\mathbf{B}$	=	state-space model matrices
a_M	=	missile lateral acceleration
a_T	=	target lateral acceleration
C_{L_α}	=	lift coefficient slope
c_1, c_3	=	terminal states weight parameters
H	=	Hamiltonian
H_i	=	time varying integrals
J	=	cost function
L	=	lift force
m	=	mass
N_{ZEAE}	=	zero effort angle error guidance gain
$\hat{N}_{\text{ZEAE}}$	=	predicted zero effort angle error guidance gain
N_{ZEM}	=	zero effort miss guidance gain
$\hat{N}_{\text{ZEM}}$	=	predicted zero effort miss guidance gain
$\mathbf{Q}_f$, $\mathbf{Q}$, $\mathbf{R}$	=	cost function weight matrices
r	=	range between target and missile
S	=	reference area
t_f	=	time of intercept
$\hat{t}_f$	=	predicted time of intercept
t_{go}	=	time to go
u	=	control input/guidance command
u^*	=	optimal controller/guidance command
u_{lim}	=	time varying acceleration constraint function
$\hat{u}_{\text{lim}}$	=	predicted time varying acceleration constraint function
u_{lim_i}	=	ith iteration time varying acceleration constraint function
V_M	=	missile speed
V_r	=	radial speed
V_T	=	target speed
V_θ	=	angular speed
$\mathbf{x}$	=	state vector
x_i	=	ith state of state vector $\mathbf{x}$
z	=	relative displacement between target and initial line of sight
α	=	angle of attack
γ_I^C	=	terminal intercept angle constraint
γ_I	=	intercept angle
γ_M	=	missile path angle
γ_T	=	target path angle
$\overline{\Delta u_{\text{lim}}}$	=	mean difference between consecutive time varying acceleration constraint computations
Δx_3	=	terminal intercept angle error
θ	=	line-of-sight angle
λ_i	=	adjoint parameters
ρ	=	air density
τ	=	autopilot time constant
ϕ	=	angle between velocity and line of sight
ψ_i	=	time varying functions

I. Introduction

THERE are various scenarios in which endoatmospheric missiles are subject to substantial aerodynamic pressure variation due to altitude and/or speed change. These may include ballistic missile interceptors, launched from the ground or from the air, toward a ballistic missile in its initial boosting phase or its terminal reentry phase. It may also be encountered by long range air-to-ground or ground-to-ground missiles that reach high altitude before entering the endgame maneuver.

Aerodynamic steering missiles are usually maneuver limited due to a maximal allowable angle of attack (AOA), sustainable by their control systems. There are also structural load limits which are common to all types of missiles. When such missiles operate in a changing environment as previously described, they are subject to a trajectory-dependent lateral acceleration constraint. Cho et al. [1] have suggested the use of a time varying weight function composed

Presented as Paper 2012-4472 at the AIAA Guidance Navigation and Control Conference, Minneapolis, 13–16 August 2012; received 30 May 2012; revision received 1 September 2012; accepted for publication 20 September 2012; published online 26 February 2013.

*Graduate Student, Department of Aerospace Engineering; itaub@iai.co.il.

†Associate Professor, Department of Aerospace Engineering; tal.shima@technion.ac.il. Associate Fellow AIAA.

of the air density and the missile's speed, for the optimal trajectory shaping of such missiles. Their goal was either to reduce the induced drag due to the missile's maneuver or to prevent command saturation in case the available acceleration was marginal. A similar attempt has been made by Shima and Shinar in [2] for a pursuit-evasion game of missiles with time varying control bounds. In both of these works, the analytical solution was obtained for an arbitrary control bound function, though the examples given assumed a simplistic linear behavior. Providing such a function for fully detailed atmospheric and aerodynamic models is quite difficult and remains an open issue. The problem becomes even more complicated when a terminal intercept angle constraint (TIAC) is introduced. The TIAC is referred to in this paper as the path angle, which is the angle between the velocities of the missile and target, rather than the attitude [3], which is the angle between the bodies of the missile and target.

Controlling the engagement geometry of a guided missile has become a growing requirement in recent years and has been addressed in numerous works [3–25]. Allowing the missile to attack its target from a specific direction holds the advantages of improving kill performance, providing penetration capabilities, reducing the warhead size, reducing collateral damage, and avoiding obstacles. The TIAC usually creates a maneuver that initially steers the missile away from a collision course with its target and later steers it back, resulting in the desired engagement geometry [9,14,15,22,23,26]. Such a maneuver is characterized by larger acceleration demands because a heading error is deliberately increased along the missile's trajectory, up to a certain point. Kim et al. [7] have shown that the capture zone, defined by the initial and final (desired) missile-target geometry, is reduced with bounded control. They have also provided an analytical computation of this zone when using a biased proportional navigation guidance law with constant control bounds. If the control bounds are trajectory dependent, as in the case of interest, the capture zone changes along the trajectory and cannot be analytically computed in advance. More important, as the control bounds change along the resulting trajectory, the missile may be lead into a no-capture zone.

If the control bounds change monotonically along the trajectory, it may be possible to avoid entering a no-capture zone by focusing the control effort either early or late, as was suggested in [12,13,16,25]. However, because these methods do not explicitly take into account the varying control bounds, and rather use design parameters for controlling the timing of the effort, they would require empirical calibration for each individual scenario. Furthermore, a combination of a large heading error and a TIAC may produce extremely curved, even S-shaped trajectories. When these trajectories also include substantial altitude and/or speed variation, the control bounds may not change monotonically and the attempt to avoid a no-capture zone by these methods may not succeed.

Several suboptimal nonlinear numerical-based methods [19,21,24] have been proposed for solving the TIAC problem. Lukacs and Yakimenko [19] have provided a trajectory shaping scheme which does not compromise the constraints on the controls, for a fully detailed kinematics model including atmosphere, aerodynamics, thrust, and gravity effects. Although these types of solutions do allow solving the problem at hand, in order to obtain a feedback-type command the scheme requires continuous real-time updating of the numerical solution. Such a computation may be too demanding for the missile's onboard CPU, and it is also relatively complicated to implement, which would require extensive and time consuming validation.

In this paper, a closed-form suboptimal guidance scheme is proposed for a missile with an arbitrary time varying acceleration constraint (TVAC), which enables the shaping of a trajectory for avoiding no-capture zones while fulfilling the guidance goal. The suggested scheme, which is based on linear quadratic (LQ) optimization, is derived for a missile with high-order autopilot dynamics, against a moving and maneuvering target, and subject to a TIAC. The TVAC is predicted using a simple and computationally affordable iterative numerical procedure, which provides time varying guidance gains for a feedback-type command, making it relatively easy to validate. The paper is organized as follows: in the next section, the kinematics of the guidance problem is presented. The derivation of the optimal guidance law is presented in Sec. III. In Sec. IV, an analytical analysis of the derived law is performed. Section V describes the computation of the expected TVAC. In addition, implementation problems are discussed, and a decomposition of the optimization is presented and analyzed. A simulation study is presented in Sec. VI. In Sec. VII, the feasibility and the optimality of the solution is evaluated, followed by conclusions in Sec. VIII.

II. Model Formulation

The engagement geometry is shown in Fig. 1 in respect to a Cartesian inertial reference frame $X_I - O_I - Z_I$. The missile and target are denoted by the subscripts M and T, respectively. The speed, lateral acceleration, and path angle are denoted by V, a, and γ, respectively. The distance between the missile and target is denoted by r, and the angle between X_I and the line of sight (LOS) is denoted by θ. The $X - O_I - Z$ frame will be used to linearize the equations of motion, where X is aligned with the initial LOS, denoted by LOS_0. The relative displacement between the target and LOS_0 is denoted by z. The missile and target accelerations normal to LOS_0 are denoted by a_{M_N} and a_{T_N}, respectively. The intercept angle is given by $\gamma_M + \gamma_T$ and is denoted as γ_I. The gravitational force is neglected. This model is based on the work of Shaferman and Shima in [23].

A. Nonlinear Kinematics

The engagement kinematics within the reference frame are given by

$$\dot{\theta} = \frac{1}{r}[-V_M \sin(\phi_M) + V_T \sin(\phi_T)] \triangleq \frac{V_\theta}{r} \tag{1}$$

$$\dot{r} = -[V_M \cos(\phi_M) + V_T \cos(\phi_T)] \triangleq V_r \tag{2}$$

where

$$\phi_M \triangleq \gamma_M - \theta \tag{3}$$

$$\phi_T \triangleq \gamma_T + \theta \tag{4}$$

The rates of the relative displacement and the intercept angle are

$$\dot{z} = V_r \sin(\theta - \theta_0) + V_\theta \cos(\theta - \theta_0) \tag{5}$$

$$\dot{\gamma}_I = \frac{a_M}{V_M} + \frac{a_T}{V_T} \tag{6}$$

Assuming the missile's autopilot dynamics can be approximated by a linear system,

$$\dot{\mathbf{x}}_M = \mathbf{A}_M \mathbf{x}_M + \mathbf{B}_M u \tag{7}$$

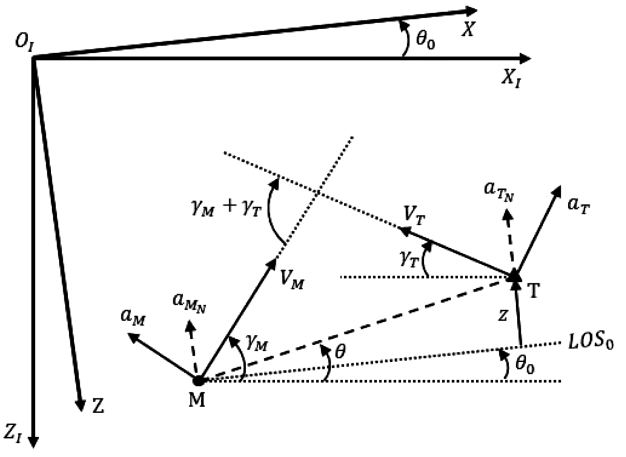

Fig. 1 Planar engagement geometry.

where $\mathbf{x}_M$ is the state vector of the autopilot variables with dim $(\mathbf{x}_M) = n$ and u is the guidance command. The lateral acceleration is given by

$$a_M = \mathbf{C}_M \mathbf{x}_M + d_M u \tag{8}$$

The target is assumed to have perfect dynamics.

B. Linearized Kinematics

Assuming the missile and the target are making small deviations around the collision course, the difference between the momentary LOS angle and its initial value can be considered small: $\theta - \theta_0 \ll 1$, in which case the dynamic model can be linearized as follows:

$$z \approx (\theta - \theta_0) r \tag{9}$$

$$\dot{z} \approx V_r(\theta - \theta_0) + V_\theta \tag{10}$$

$$\ddot{z} \approx a_T \cos \phi_{T_0} - a_M \cos \phi_{M_0} \tag{11}$$

The state-space representation of the problem is given by

$$\dot{\mathbf{x}} = \mathbf{A}\mathbf{x} + \mathbf{B}u, \qquad \mathbf{x} = [z \quad \dot{z} \quad \gamma_I \quad a_T \quad \mathbf{x}_M^T]^T \tag{12}$$

where

$$\dot{\mathbf{x}} = \begin{cases} \dot{x}_1 = x_2 \\ \dot{x}_2 = a_T \cos \phi_{T_0} - a_M \cos \phi_{M_0} \\ \dot{x}_3 = a_T/V_T + a_M/V_M \\ \dot{x}_4 = 0 \\ \dot{\mathbf{x}}_M = \mathbf{A}_M \mathbf{x}_M + \mathbf{B}_M u \end{cases}, \qquad \mathbf{A} = \begin{bmatrix} \mathbf{A}_k & \mathbf{A}_{12} \\ [0]_{nx4} & \mathbf{A}_M \end{bmatrix},$$

$$\mathbf{B} = \begin{bmatrix} 0 \\ -d_M \cos \phi_{M_0} \\ d_M/V_M \\ 0 \\ \mathbf{B}_M \end{bmatrix} \tag{13}$$

and

$$\mathbf{A}_k = \begin{bmatrix} 0 & 1 & 0 & 0 \\ 0 & 0 & 0 & \cos \phi_{T_0} \\ 0 & 0 & 0 & 1/V_T \\ 0 & 0 & 0 & 0 \end{bmatrix}, \qquad \mathbf{A}_{12} = \begin{bmatrix} [0]_{1xn} \\ -\mathbf{C}_M \cos \phi_{M_0} \\ \mathbf{C}_M/V_M \\ [0]_{1xn} \end{bmatrix} \tag{14}$$

with [0] denoting a matrix of zeros with appropriate dimensions.

III. Guidance Law Derivation

A. Time Varying Acceleration Constraint Cost Function

In LQ optimization, the cost function to be minimized is of the form

$$J = \frac{1}{2}\mathbf{x}^T(t_f)\mathbf{Q}_f\mathbf{x}(t_f) + \frac{1}{2}\int_{t_0}^{t_f} [\mathbf{x}^T\mathbf{Q}\mathbf{x} + u^T\mathbf{R}u]\mathrm{d}\xi \tag{15}$$

where $\mathbf{Q}_f$, $\mathbf{Q}$, and $\mathbf{R}$ are weight functions.

If the control weight function $\mathbf{R}$ is chosen as constant, the control u is given a unified weight throughout the engagement. In the case of a TVAC, it is preferable to avoid saturation where possible, that is, avoid issuing guidance commands which are larger than the momentary available lateral acceleration. For this purpose, the following weight function is used, for a single input system, which is the basis of the TVAC trajectory shaping guidance law:

$$\mathbf{R} = \frac{1}{u_{\lim}^2(t)} \tag{16}$$

where $u_{\lim}(t)$ is the TVAC.

This means that the penalty for maneuvering is higher where the acceleration constraint is lower, throughout the engagement. The optimal guidance command would be that which minimizes the terminal and running states and at the same time generates commands that are as small as possible, relative to the TVAC.

It should be noted that the proposed TVAC optimization is not restricted to TIAC guidance problems alone and can be used in any guidance/control problem, where needed, as long as it is treated within an LQ optimization framework.

B. Optimal Controller

The optimal guidance law for the terminal intercept angle problem with TVACs will be derived in the following subsection. For the sake of simplicity, and without sacrificing generality, the guidance law will be demonstrated for a missile with first-order autopilot dynamics, in which case the model is reduced to

$$\mathbf{x}_M = a_M, \qquad \mathbf{A}_M = -1/\tau, \qquad \mathbf{B}_M = 1/\tau, \qquad \mathbf{C}_M = 1, \qquad d_M = 0 \tag{17}$$

where τ is the autopilot time constant.

The cost function to be minimized is given by

$$J = \frac{c_1}{2}x_1^2(t_f) + \frac{c_3}{2}\Delta x_3^2(t_f) + \frac{1}{2}\int_{t_0}^{t_f} \frac{u^2(\xi)}{u_{\lim}^2(\xi)}\,\mathrm{d}\xi \tag{18}$$

where

$$\Delta x_3(t_f) \triangleq x_3(t_f) - \gamma_I^C \tag{19}$$

and γ_I^C is the TIAC.

The Hamiltonian of the problem is

$$H = \lambda_1 x_2 + \lambda_2(x_4 \cos \phi_{T_0} - x_5 \cos \phi_{M_0}) + \lambda_3(x_4/vT + x_5/v_M) + \lambda_5 \frac{u - x_5}{\tau} + \frac{1}{2}\frac{u^2}{u_{\lim}^2} \tag{20}$$

The optimal controller satisfies $u^* = \arg_u \min H$, therefore

$$u^* = -\frac{\lambda_5}{\tau}u_{\lim}^2 \tag{21}$$

The adjoint equations are

$$\begin{cases} \dot{\lambda}_1 = -\frac{\partial H}{\partial x_1} = 0 & \lambda_1(t_f) = c_1 x_1(t_f) \\ \dot{\lambda}_2 = -\frac{\partial H}{\partial x_2} = -\lambda_1 & \lambda_2(t_f) = 0 \\ \dot{\lambda}_3 = -\frac{\partial H}{\partial x_3} = 0 & \lambda_3(t_f) = c_3\Delta x_3(t_f) \\ \dot{\lambda}_5 = -\frac{\partial H}{\partial x_5} = \lambda_2 \cos \phi_{M_0} - \frac{\lambda_3}{V_M} + \frac{\lambda_5}{\tau} & \lambda_5(t_f) = 0 \end{cases}, \tag{22}$$

with the solutions

$$\begin{cases} \lambda_1(t) = c_1 x_1(t_f) \\ \lambda_2(t) = c_1 x_1(t_f)(t_f - t) \\ \lambda_3(t) = c_3\Delta x_3(t_f) \\ \lambda_5(t) = -c_1\tau^2\psi_1(\zeta)x_1(t_f)\cos \phi_{M_0} - c_3\tau\psi_2(\zeta)\Delta x_3(t_f)/V_M \end{cases} \tag{23}$$

where

$$\psi_1(\zeta) \triangleq e^{-\zeta} + \zeta - 1, \qquad \psi_2(\zeta) \triangleq e^{-\zeta} - 1, \qquad \zeta \triangleq \frac{t_f - t}{\tau} \tag{24}$$

Substituting Eq. (23) into Eq. (21) provides

$$u^* = u_{\lim}^2[c_1\tau\psi_1(\zeta)x_1(t_f) + c_3\psi_2(\zeta)\Delta x_3(t_f)/V_M] \tag{25}$$

Integrating Eq. (12) from t to t_f yields two coupled algebraic equations:

$$\begin{aligned} x_1(t_f) &= \text{ZEM} - c_1\cos^2\phi_{M_0}x_1(t_f)H_1(t) - c_3\frac{\Delta x_3(t_f)}{V_M}H_{12}(t) \\ \Delta x_3(t_f) &= \text{ZEAE} - c_1\frac{\cos\phi_{M_0}}{V_M}x_1(t_f)H_{12}(t) - c_3\frac{\Delta x_3(t_f)}{V_M^2}H_2(t) \end{aligned} \tag{26}$$

where the zero effort miss (ZEM) and the zero effort angle error (ZEAE) are the expected intercept errors for a zero guidance command, given by

$$\begin{aligned} \text{ZEM} &\triangleq x_1(t) + t_{\text{go}}x_2(t) + \frac{t_{\text{go}}^2}{2}\cos\phi_{T_0}x_4(t) - \tau^2\psi_1(\zeta)\cos\phi_{M_0}x_5(t) \\ \text{ZEAE} &\triangleq x_3(t) + t_{\text{go}}\frac{x_4(t)}{V_T} - \tau\psi_2(\zeta)\frac{x_5(t)}{V_M} - \gamma_I^C \end{aligned} \tag{27}$$

The terms H_1, H_{12}, and H_2 are the time varying integrals:

$$\begin{aligned} H_1(t) &\triangleq \int_t^{t_f}\tau^2\psi_1^2u_{\lim}^2\,\mathrm{d}\xi \\ H_{12}(t) &\triangleq \int_t^{t_f}\tau\psi_1\psi_2u_{\lim}^2\,\mathrm{d}\xi \\ H_2(t) &\triangleq \int_t^{t_f}\psi_2^2u_{\lim}^2\,\mathrm{d}\xi \end{aligned} \tag{28}$$

Extracting the terminal states from Eq. (26) yields

$$x_1(t_f) = \frac{(V_M^2 + c_3H_2(t))\text{ZEM} - c_3\cos\phi_{M_0}V_MH_{12}(t)\text{ZEAE}}{(c_1\cos^2\phi_{M_0}H_1(t) + 1)V_M^2 + c_1c_3\cos^2\phi_{M_0}(H_1(t)H_2(t) - H_{12}^2(t)) + c_3H_2(t)} \tag{29}$$

$$\Delta x_3(t_f) = -V_M\frac{c_1\cos\phi_{M_0}H_{12}(t)\text{ZEM} - V_M(c_1\cos^2\phi_{M_0}H_1(t) + 1)\text{ZEAE}}{(c_1\cos^2\phi_{M_0}H_1(t) + 1)V_M^2 + c_1c_3\cos^2\phi_{M_0}(H_1(t)H_2(t) - H_{12}^2(t)) + c_3H_2(t)} \tag{30}$$

Substituting Eqs. (29) and (30) into Eq. (25) yields

$$\begin{aligned} u^*(t) = u_{\lim}^2(t)&\frac{c_1\cos\phi_{M_0}[\tau\psi_1(\zeta)(c_3H_2(t) + V_M^2) - c_3\psi_2(\zeta)H_{12}(t)]\text{ZEM}}{(c_1\cos^2\phi_{M_0}H_1(t) + 1)V_M^2 + c_1c_3\cos^2\phi_{M_0}(H_1(t)H_2(t) - H_{12}^2(t)) + c_3H_2(t)} - \\ u_{\lim}^2(t)&\frac{c_3V_M[c_1\tau\psi_1(\zeta)\cos^2\phi_{M_0}H_{12}(t) - \psi_2(\zeta)(c_1\cos^2\phi_{M_0}H_1(t) + 1)]\text{ZEAE}}{(c_1\cos^2\phi_{M_0}H_1(t) + 1)V_M^2 + c_1c_3\cos^2\phi_{M_0}(H_1(t)H_2(t) - H_{12}^2(t)) + c_3H_2(t)} \end{aligned} \tag{31}$$

For a perfect intercept and a perfect intercept angle, the weights will be given infinite values: $c_1, c_3 \to \infty$, yielding

$$u^*(t) = \frac{1}{\cos\phi_{M_0}}\frac{N_{\text{ZEM}}}{t_{\text{go}}^2}\text{ZEM} + \frac{N_{\text{ZEAE}}}{t_{\text{go}}}V_M\text{ZEAE} \tag{32}$$

where N_{ZEM} and N_{ZEAE} are the time varying guidance gains, given by

$$\begin{aligned} N_{\text{ZEM}}(t) &= u_{\lim}^2(t)t_{\text{go}}^2\frac{\tau\psi_1(\zeta)H_2(t) - \psi_2(\zeta)H_{12}(t)}{H_1(t)H_2(t) - H_{12}^2(t)} \\ N_{\text{ZEAE}}(t) &= u_{\lim}^2(t)t_{go}\frac{\psi_2(\zeta)H_1(t) - \tau\psi_1(\zeta)H_{12}(t)}{H_1(t)H_2(t) - H_{12}^2(t)} \end{aligned} \tag{33}$$

Using the linear approximation of Eqs. (9) and (10), and assuming the time to go can be approximated by $t_{\text{go}} \approx -\frac{r}{V_r}$, the first two terms of the ZEM expression can be written as

$$\begin{aligned} x_1(t) + t_{\text{go}}x_2(t) &= z + t_{\text{go}}\dot{z} = (\theta - \theta_0)r + t_{\text{go}}V_r(\theta - \theta_0) \\ &+ t_{\text{go}}V_\theta = -V_rt_{\text{go}}^2\dot{\theta} \end{aligned} \tag{34}$$

Therefore, the ZEM can be written as

$$\text{ZEM} = -V_rt_{\text{go}}^2\dot{\theta} + a_T\cos\phi_{T_0}\frac{t_{\text{go}}^2}{2} - a_M\cos\phi_{M_0}\tau^2\psi_1(\zeta) \tag{35}$$

The ZEAE is simply

$$ZEAE = (\gamma_I - \gamma_I^C) + t_{go}\frac{a_T}{V_T} - \frac{a_M}{V_M}\tau\psi_2(\zeta) \tag{36}$$

IV. Guidance Law Study

This section discusses the resulting guidance law. The effects of the TVAC and the autopilot dynamics will be examined, separately and combined, followed by conclusions. The study will be conducted for the case of a perfect intercept and a perfect intercept angle, that is, $c_1, c_3 \to \infty$.

A. Constant Acceleration Constraint Without Autopilot Dynamics

For the purpose of understanding the derived guidance law, it will be reduced to its simplest form and then rebuilt from there on. First, it will be assumed that the weight function R is constant and equal to 1, that is to say, the TVAC is ignored and assumed constant. It will be further assumed that the missile has perfect dynamics, that is, $\tau \to 0$. Under these assumptions, the time varying ψ functions are

$$\lim_{\tau\to 0}\tau\psi_1(\zeta) = t_{\text{go}} \quad \lim_{\tau\to 0}\psi_2(\zeta) = -1 \tag{37}$$

in which case the integrals H_1, H_{12}, and H_2 are

$$H_1 = \frac{1}{3}t_{\text{go}}^3 \quad H_{12} = -\frac{1}{2}t_{\text{go}}^2 \quad H_2 = t_{\text{go}} \tag{38}$$

and the constants in these equations have the appropriate units. The resulting guidance gains are reduced to

$$N_{\text{ZEM}} = 6 \quad N_{\text{ZEAE}} = 2 \tag{39}$$

The terms related to the missile's own lateral acceleration within the expressions of ZEM and ZEAE are removed all together, giving us the exact same optimal guidance law obtained in [23]. The guidance command with the gains of Eq. (39) will be denoted from here on as the constant acceleration constraint (CAC), or u_{CAC}^*. In the following figures, the gains of the different cases will be normalized by their CAC values, i.e., by 6 for N_{ZEM} and by 2 for N_{ZEAE}.

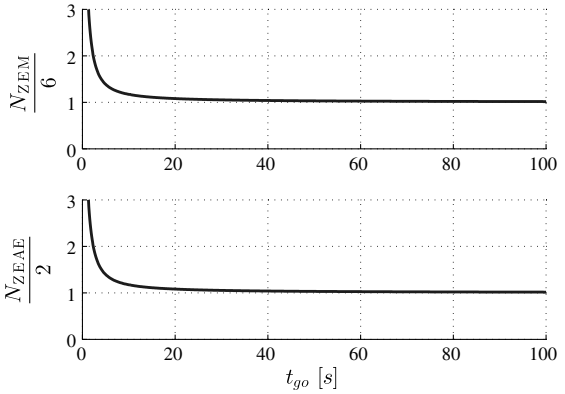

Fig. 2 CACD gains.

It is noted that if the TIAC is not imposed ($c_3 \to 0$) the gains N_{ZEM} and N_{ZEAE} become 3 and 0, respectively, which is a well-known optimal augmented proportional navigation guidance law.

B. Constant Acceleration Constraint with Autopilot Dynamics

The effect of the autopilot dynamics, or lag, is shown in Fig. 2 for $\tau = 0.5$ s, assuming $u_{\text{lim}} = 1$. The resulting guidance command will be denoted from here on as constant acceleration constraint with dynamics (CACD), or u^*_{CACD}.

The autopilot lag causes a delay between the guidance command and the actual lateral acceleration. This in return deteriorates the guidance performance, because the required lateral acceleration near intercept is unmet. The optimization produces guidance gains that increase to infinity as $t_{\text{go}} \to 0$, expediting the autopilot near intercept in order to overcome the effect of the lag. This increase is timed so that the actual acceleration, given the lag, would be as required in order to minimize the cost function. For $t_{\text{go}} \to \infty$ (which is mathematically similar to $\tau \to 0$), the guidance gains are constant and equal in value to those without autopilot lag, suggesting that for large values of t_{go} the effect of the autopilot lag is negligible.

Higher-order autopilot dynamics would introduce additional terms to the ZEM and ZEAE expressions given in Eqs. (35) and (36). The expressions of the H_1, H_{12}, and H_2 integrals given in Eq. (28) and the guidance gains given in Eq. (33) will be different as well. However, as was shown in [27] the effect of the autopilot lag on the guidance gains, for any order, would maintain the preceding characteristics for $t_{\text{go}} \to 0$ and $t_{\text{go}} \to \infty$. The main difference would be in small and finite values of t_{go}, e.g., an inverse response in the case of a nonminimum phase system.

C. Time Varying Acceleration Constraint Without Autopilot Dynamics

Figure 3 displays the gains of a linear and a parabolic TVAC, without autopilot dynamics. The resulting guidance command will be denoted from here on as TVAC without dynamics, or u^*_{TVAC}. In one case, shown in Fig. 3a, the TVAC has an initial value that is lower than the final value, referenced as "Increasing." In another case, shown in Fig. 3b, the TVAC has an initial value that is higher than the final value, referenced as "Decreasing."

Analyzing the gain profiles, the following heuristic conclusions will be offered:

1) The TVAC optimization provides a guidance law in which the authority to maneuver[‡] depends on the available lateral acceleration. If, for instance, the available acceleration is initially high and decreases with time, the authority to maneuver will be initially high as well and decrease with time. This in return would cause the missile to maneuver early and position itself near the collision course and near the required intercept angle, while it is still capable of maneuvering. This would also require less maneuvering later, when it is less maneuver capable.

2) The authority to maneuver is not unified across the guidance command terms. This is because each command term has a different long-term effect on the guidance command magnitude; the intercept angle term ZEAE, which causes a deviation from the collision course, has an increasing effect on the required acceleration, whereas the ZEM term, which reduces this deviation, has a decreasing effect. This behavior can be seen quite clearly in three of the examples:

a) Increasing TVAC: in both cases (linear and parabolic), the initial relatively higher value of N_{ZEM} keeps the missile closer to the collision course, and only later, when it has more maneuverability, is it allowed to correct the intercept angle as well.

b) Parabolic decreasing TVAC: both gains are initially relatively higher, which is similar to the case of the linear decreasing TVAC. However, because of the "choking" point near intercept, where the TVAC reaches a minimal value, the gain N_{ZEM} becomes at some point relatively higher than N_{ZEAE}, which brings the missile closer to the collision course and reduces the required maneuverability later. For this reason, N_{ZEAE} is initially relatively higher than N_{ZEM}, as it compensates for the lack of intercept angle correction near the end of the engagement.

The behavior described previously is the result of the TVAC being a part of the running cost. This allows taking into account the available acceleration throughout the engagement with appropriate planning.

D. Time Varying Acceleration Constraint with Autopilot Dynamics

Figure 4 shows the gains with autopilot dynamics for the case of the parabolic decreasing TVAC, $\tau = 0.5$ s. The TVAC guidance command with autopilot dynamics will be denoted from here on as u^*_{TVACD}. In the same figure are also the CACD and TVAC gains. For large values of t_{go}, the gains of TVACD seem almost identical to those of TVAC, whereas, for small values of t_{go}, the gains of TVACD seem almost identical to those of CACD.

This behavior suggests that the influence of the autopilot dynamics on the optimal gains seems to be somewhat independent of the TVAC, which leads to the assumption that the optimization may be separated. This hypothesis will be examined in Sec. V.C, in which it will be used to overcome implementation problems.

V. Implementation

A. Computation of the Time Varying Acceleration Constraint

As was explained in the introduction, aerodynamic steering missiles are usually subject to an AOA limitation, whether constant or time varying, depending on the autopilot's ability to maintain dynamic stability. Their lateral acceleration is achieved by a lift force, which is a function of the dynamic pressure and the AOA:

$$m \cdot a_M = L = \frac{1}{2}\rho V_M^2 S C_{L_\alpha} \alpha \tag{40}$$

where m is the missile's mass, ρ is the air density, V is the missile's speed, S is the reference area, C_{L_α} is the lift coefficient slope, and α is the AOA.

When the acceleration limit in Sec. III.A was defined as a time-dependent function, it allowed obtaining the simple feedback-type guidance command given in Eq. (32). However, from Eq. (40) it is clear that this definition is inaccurate, because the actual acceleration constraint for a given AOA limit would be

$$u_{\text{lim}} = \frac{1}{2}\frac{\rho V_M^2 S C_{L_\alpha}}{m}\alpha_{\text{lim}} \tag{41}$$

Finding a simple feedback-type solution for the accurate constraint given in Eq. (41) would be difficult, if not impossible, because of the nonlinear behavior of the various elements comprising this constraint. Although the definition of the acceleration constraint as being time dependent rather than state dependent has allowed overcoming this problem, it raised a different one: the relationship

[‡]A feedback-type command is composed of errors multiplied by gains. The gains determine the proportion between the command and the error, or, in other words, the gains represent the authority to correct the error; infinite gains mean unlimited authority, and zero gains mean no authority whatsoever.

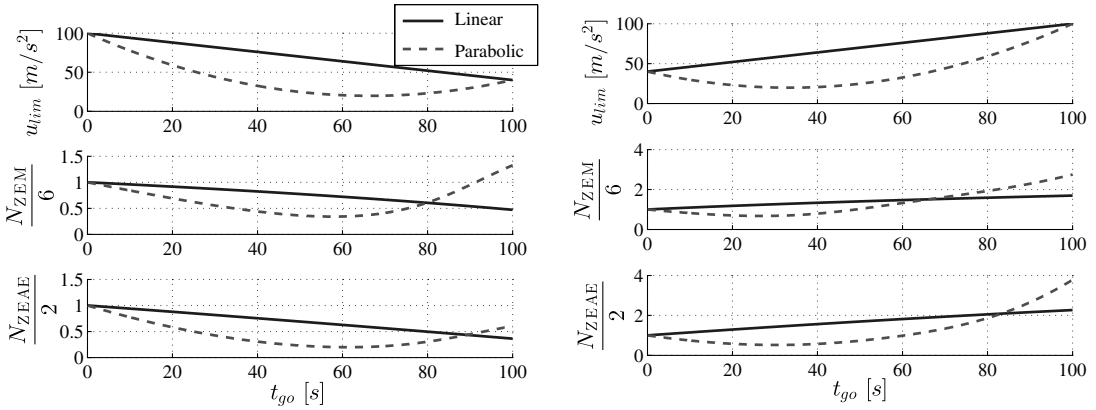

a) Increasing TVAC **b) Decreasing TVAC**

Fig. 3 TVAC gains without autopilot dynamics ($\tau = 0$).

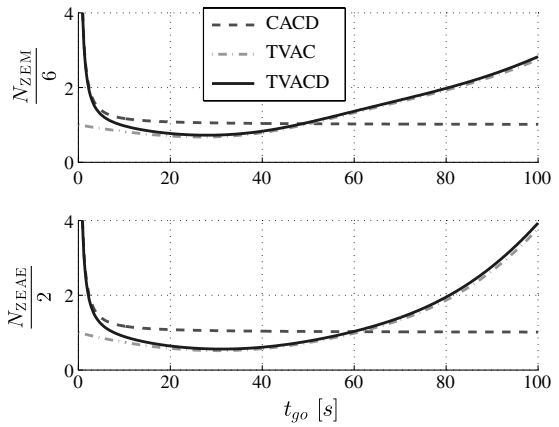

Fig. 4 TVACD gains, parabolic decreasing TVAC.

between the acceleration constraint and time must be found in order to obtain a closed-form solution. Finding this relationship is difficult because of the interaction between the guidance command and the various elements, described as follows.

In the scenarios of interest, in which endoatmospheric missiles are subject to a substantial altitude variation, the air density varies substantially as well. As the missile maneuvers, it is subject to a drag force, which together with gravity changes its speed. This means that the lateral acceleration constraint, which for a given AOA limit is a function of the dynamic pressure, is also a function of the trajectory. The trajectory itself is the result of the TVAC guidance law, which is a function of the TVAC constraint:

$$[\rho V_M]^T = f_1(u,t), \qquad u = f_2(\mathbf{x}, V_M, u_{\rm lim}), \qquad u_{\rm lim} = f_3(\rho, V_M) \tag{42}$$

Because the relations between these elements are nonlinear it would be, again, very difficult, if not impossible, to analytically predict the TVAC. To solve this enigmatic problem, the following numerical iterative procedure is proposed for the prediction of the TVAC along the expected trajectory:

1) Using the fully detailed atmospheric and aerodynamic models, make an initial guess of the TVAC function, including the expected engagement duration $\hat{t}_f$. It could be a constant or a more ingenious guess such as a linear function based on initial (known) and expected final conditions (design requirements, scenario terminal constraints, etc).

2) Calculate the time varying guidance gains in Eq. (33) for the given TVAC function and the predicted $\hat{t}_f$. As will be explained in the following steps, the TVAC function will be discrete; therefore, the H_1, H_{12}, and H_2 integrals will be calculated numerically (e.g., trapezoid integration). Alternatively, the discrete TVAC can be approximated by a polynom, and the integrals can be obtained analytically. For each instance t, starting from $t = 0$ and up to $t = \hat{t}_f$, the values of the guidance gains for this instance are obtained by integrating H_1, H_{12}, and H_2 from t to $\hat{t}_f$. Note that, when $u_{\rm lim}(t)$ and $\hat{t}_t$ are given, calculating the guidance gains as functions of time is straightforward and explicit, and no additional information is needed. This is because the varying acceleration constraint is assumed to be an explicit function of time, which is not affected by the actual trajectory or speed.

3) Run a simple three-degree-of-freedom (DOF) nonlinear point-mass simulation using the TVAC optimized guidance command in Eq. (32) and the precalculated gains of step 2. The ZEM and the ZEAE are calculated at each step of the simulation for the momentary state. If the actual engagement time is longer than $\hat{t}_f$, freeze the values of the gains at some minimal value of $t_{\rm go}$, and use these constant values until intercept is achieved or until the missile passes the target. Keep updating the ZEM and ZEAE while the gains are frozen.

4) Along the resulting trajectory, calculate and record the actual TVAC using the aforementioned detailed models. This calculation will also be used during the simulation to constrain the guidance command and avoid reaching an AOA that is larger than the limit. Note that by using a fully detailed nonlinear simulation as suggested a realistic physical behavior can be obtained, as all the relevant forces (thrust, drag, lift, and gravity) are simulated.

5) Repeat steps 2–4 while updating the TVAC and the guidance gains between iterations, until a final condition has been met. The final condition could be, for instance, a convergence in the overall error between consecutive TVACs or the achievement of the guidance goal. If the first criterion is chosen, it is expected that the predicted TVAC would match the actual TVAC along the resulting trajectory, which is a desired result.

B. Open-Loop Guidance Gains Computation

Once the predicted TVAC function $\hat{u}_{\rm lim}(t)$ has been obtained, where $t \in [0, \hat{t}_f]$, the guidance gains can be calculated in advance from $t = 0$ to $t = \hat{t}_f$ using Eq. (33). In fact, this has already been done at the beginning of each iteration of the procedure described in Sec. V.A. Suppose $\hat{u}_{\rm lim}$ is the parabolic decreasing function given in Fig. 3b. According to the prediction, the predicted time of intercept, $\hat{t}_f$, is 100 s. At $t = 20$ s ($\hat{t}_{\rm go} = 80$ s), the precalculated gains $\hat{N}_{\rm ZEM}$ and $\hat{N}_{\rm ZEAE}$ should be approximately 12 and 4, respectively. At $t = 100$ s ($\hat{t}_{\rm go} = 0$ s), their values should be 6 and 2. The precalculated gains are used with the optimal guidance command given in Eq. (32), whereas the remaining terms, including the guidance errors ZEM and ZEAE, are measured or estimated in real time. This means that the guidance gains are scheduled in an open loop, but the guidance command remains of feedback type:

$$u(t) = \frac{1}{\cos\phi_{M_0}} \frac{\hat{N}_{\rm ZEM}}{t_{\rm go}^2} {\rm ZEM} + \frac{\hat{N}_{\rm ZEAE}}{t_{\rm go}} V_M {\rm ZEAE} \tag{43}$$

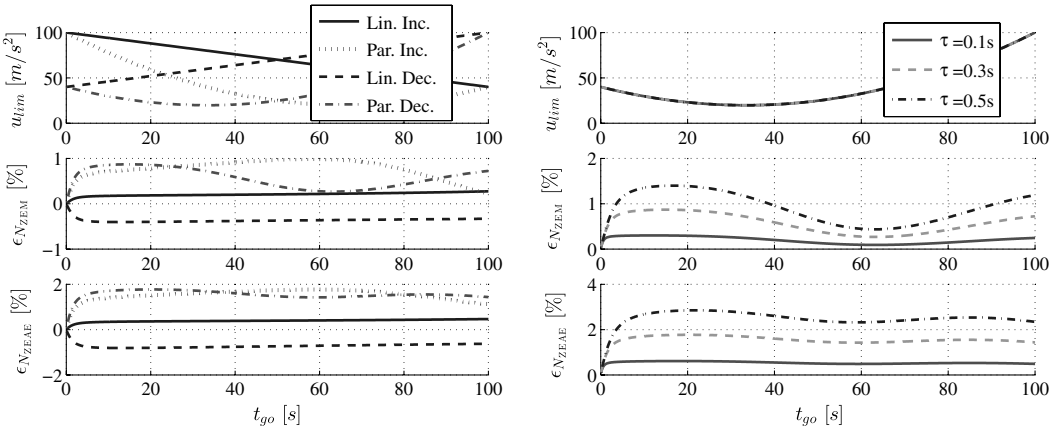

a) Various TVAC examples, τ = 0.5*s* **b) Autopilot time constant effect**

Fig. 5 Decomposed gains errors.

where

$$\hat{N}_{(\cdot)} = N_{(\cdot)}(\hat{t}_f - t, \hat{u}_{\lim}) \tag{44}$$

The fact that the guidance command remains of feedback type makes it robust against model uncertainties and external disturbances, up to a certain extent. If the uncertainties and the disturbances are substantial, the actual trajectory and the resulting TVAC may change substantially as well, and the current predicted TVAC would produce inadequate trajectory shaping. This problem may be overcome by providing an observer; i.e., periodically update the TVAC prediction by running the iterative procedure described in Sec. V.A, while using the feedback-type command given in Eq. (43) between updates. On the other hand, if the uncertainties and the disturbances are small enough, they can be overlooked, and the main problem to be dealt with is the fact that the actual intercept time t_f could be shorter or longer than $\hat{t}_f$, as shall be shortly explained.

When autopilot lag compensation is used, i.e., using the u^*_{TVACD} command, and the engagement is shorter than expected ($t_f < \hat{t}_f$), the gains may not rise in a proper timing before intercept and the lag would be compensated incorrectly, resulting in larger intercept errors. If the engagement is longer than expected ($t_f > \hat{t}_f$), the gains will rise too early and reach extremely large values for quite some time before intercept. Not only would the compensation of the autopilot dynamics be incorrect, this could also destabilize the system by increasing measurement noise and, again, result in larger intercept errors.

If autopilot lag compensation is not used, i.e., using the u^*_{TVAC} command, when $t_f < \hat{t}_f$ the guidance gains would be near their converged values upon intercept, and when $t_f > \hat{t}_f$ gains will be frozen at $t = \hat{t}_f$, at their converged values. Although this allows avoiding the extremely large gain problem, the autopilot lag is still not compensated.

To overcome this problem, one may suggest using a real-time calculated t_{go}, such as $-r/V_r$. Although this calculation may be accurate near intercept at small values of t_{go} (when the missile and target are on the collision course), it would be quite erroneous for large values of t_{go}, especially when imposing a TIAC. As was previously mentioned in the introduction, the TIAC usually produces a trajectory for which a heading error is initially increased. Some combinations of initial and terminal conditions could produce extremely curved trajectories, even S shaped. The calculation error of t_{go} in such trajectories could become quite large, even when using more sophisticated methods, such as the one suggested in [11]. To illustrate the effect of such an error on the TVAC gain calculation, consider a case in which the missile is initially on the collision course but not at the required intercept angle. The guidance command would steer the missile away from the collision course and increase the heading error in order to achieve the TIAC later. As the missile steers away, a calculation of t_{go} by $-r/V_r$ could produce a value that increases with time.[§] This is obviously wrong, because the actual t_{go} can only decrease with time. As a result, instead of advancing the values of the guidance gains along the predicted t_{go} scale toward $t_{\text{go}} = 0$, they are actually frozen or moving backward along this scale. This would lead to a completely wrong TVAC gain calculation, wrong trajectory shaping, subsequent command saturation, and a large miss distance.

In Sec. IV.D, it was shown that the influence of the TVAC on the optimal gains is dominant for large values of t_{go}, whereas the influence of the autopilot lag is dominant for small values of t_{go}. If the guidance command is somehow separated so that the TVAC gains are obtained using the open-loop t_{go} calculation (by $\hat{t}_f$), and the autopilot lag compensation is obtained in a closed-loop t_{go} calculation, such as $-r/V_r$, the advantage of each method can be obtained. For this purpose the following optimization decomposition is offered.

C. Optimization Decomposition

Taking advantage of the common converged gain values of u^*_{CACD} ($t_{\text{go}} \to \infty$) and u^*_{TVAC} ($t_{\text{go}} \to 0$), the following normalization can be used:

$$N_{\text{ZEM}_{\text{TVACND}}} \triangleq \frac{N_{\text{ZEM}_{\text{TVAC}}} \cdot N_{\text{ZEM}_{\text{CACD}}}}{6} = \frac{N_{\text{ZEM}_{\text{TVAC}}}}{\lim\limits_{t_{\text{go}}\to 0} N_{\text{ZEM}_{\text{TVAC}}}} \cdot N_{\text{ZEM}_{\text{CACD}}}$$

$$= N_{\text{ZEM}_{\text{TVAC}}} \cdot \frac{N_{\text{ZEM}_{\text{CACD}}}}{\lim\limits_{t_{\text{go}}\to \infty} N_{\text{ZEM}_{\text{CACD}}}}$$

$$N_{\text{ZEAE}_{\text{TVACND}}} \triangleq \frac{N_{\text{ZEAE}_{\text{TVAC}}} \cdot N_{\text{ZEAE}_{\text{CACD}}}}{2} = \frac{N_{\text{ZEAE}_{\text{TVAC}}}}{\lim\limits_{t_{\text{go}}\to 0} N_{\text{ZEAE}_{\text{TVAC}}}}$$

$$\cdot N_{\text{ZEAE}_{\text{CACD}}} = N_{\text{ZEAE}_{\text{TVAC}}} \cdot \frac{N_{\text{ZEAE}_{\text{CACD}}}}{\lim\limits_{t_{\text{go}}\to \infty} N_{\text{ZEAE}_{\text{CACD}}}} \tag{45}$$

Putting Eq. (45) into words, for large values of t_{go} the ratio $N_{\text{ZEM}_{\text{CACD}}}/6$ is nearly 1, therefore $N_{\text{ZEM}_{\text{TVACND}}}$ would be similar to $N_{\text{ZEM}_{\text{TVAC}}}$, and for small values of t_{go} the ratio $N_{\text{ZEM}_{\text{TVAC}}}/6$ is nearly 1, therefore $N_{\text{ZEM}_{\text{TVACND}}}$ would be similar to $N_{\text{ZEM}_{\text{CACD}}}$. In a similar manner, the characteristics of $N_{\text{ZEAE}_{\text{TVACND}}}$ are obtained.

Figure 5a shows the error (in percent) between the gains of TVACD and TVACND for the various TVAC examples given in Fig. 3 and for $\tau = 0.5$ s. The effect of the autopilot time constant is shown in Fig. 5b. The errors are quite small and increase with τ, which can be explained by the fact that the autopilot's lag effect on the optimal gains extends to larger values of t_{go} for a larger time constant. If the

[§]The closing velocity may decrease with the increased heading error and/or speed reduction due to maneuver and induced drag.

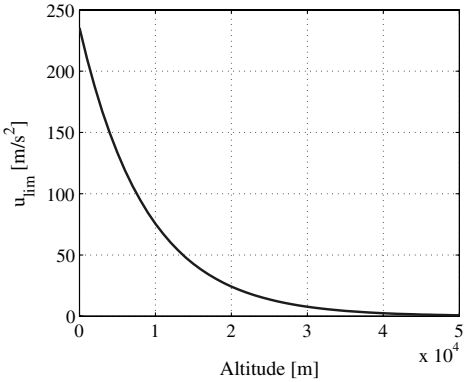

Fig. 6 Acceleration constraint.

errors remain relatively small, the resulting guidance law u_{TVACND} can be considered suboptimal.

Now that the effects of the autopilot dynamics and the TVAC trajectory shaping have been separated, the gains can be calculated separately: the gains N_{TVAC} will be calculated by the open-loop time to go ($\hat{t}_{\mathrm{go}} = \hat{t}_f - t$), and the gains N_{CACD} are calculated using the real-time time to go (such as $-r/V_r$). The decomposed guidance command will be referred to from here on as TVAC with normalized dynamics, or u_{TVACND}. It is clear that the decomposition can be used for an autopilot of any order and that the mere difference would be in the characteristics of the CACD gains for small values of t_{go} and in the error profiles shown in Fig. 5.

It is noted that for the purpose of separating the guidance gains a similar result can be obtained using the method of matched asymptotic expansions, in which the gains of u^*_{CACD} serve as the inner solution and the gains of u^*_{TVAC} are the outer solution:

$$N_{\mathrm{ZEM_{TVACAD}}} \triangleq N_{\mathrm{ZEM_{CACD}}} + N_{\mathrm{ZEM_{TVAC}}} - 6$$
$$N_{\mathrm{ZEAE_{TVACAD}}} \triangleq N_{ZEAE_{\mathrm{CACD}}} + N_{\mathrm{ZEAE_{TVAC}}} - 2 \qquad (46)$$

VI. Simulation Results

In this section, the TVAC guidance scheme performance will be examined with the aid of a nonlinear simulation, for the case of a perfect intercept ($c_1, c_3 \to \infty$). First, the properties of the optimal guidance law, which disregards the varying acceleration constraint, will be examined. Second, the proposed guidance scheme with an iterative solution of the TVAC will be demonstrated. Last, the guidance scheme's ability to cope with model uncertainties will be investigated, and the contribution of the decomposed command will be evaluated.

A. Simulation Scenario

The examination will be based on a single scenario against a constantly maneuvering target. Both the missile and target will have constant speeds, and the missile will be subject to an altitude-dependent acceleration constraint, simulating the varying dynamic pressure effect due to altitude change. A head-on intercept ($\gamma_I^C = 0°$) of a ballistic missile target will be simulated, where the interceptor is launched vertically from the ground. The interceptor and target will be moving at speeds of 900 and 700 m/s, respectively, and the target will perform a 10 m/s^2 maneuver. The altitude-dependent acceleration constraint is given in Fig. 6. Because the missile and target are not initially on a collision course, the angles ϕ_{M_0} and ϕ_{T_0} will be updated at each step of the simulation.

B. Guidance Performance, Ignoring the Varying Acceleration Limit

For the purpose of demonstrating the problem arising when the guidance disregards the varying acceleration constraint, the simulation will be run without autopilot lag, first without imposing the acceleration constraint (denoted NAC) and then with a limited guidance command (denoted CAC). The resulting trajectories and guidance commands are plotted in Fig. 7. Analyzing the results, it can be observed that the missile starts a moderate turn toward the target in order to minimize the miss distance and achieve the desired intercept angle. As it reaches an altitude at which the guidance command is higher than the available lateral acceleration, it is unable to bend its trajectory toward the target and consequentially misses by approximately 800 m.

It is noted that this problem might be addressed indirectly by using a proper combination of finite terminal weights c_1, c_3. However, such a solution has several major disadvantages:

1) Determining the weights c_1, c_3 is not straightforward; one must find a method applicable for the entire battle space, defined by a wide range of initial and final conditions.

2) Even if a solution is found, it does not necessarily provide enough AOA clearance throughout the engagement. When introducing model uncertainties such as lower density or less lift, the missile might enter a no-capture zone.

3) If guidance accuracy is a critical requirement, the use of finite weights might not allow achieving the guidance goal.

C. Time Varying Acceleration Constraint Iterative Computation, Performed by the Guidance Algorithm

In order to utilize the trajectory shaping of the TVAC guidance problem, the TVAC must be predicted first, as described in Sec. V.A. Our initial guess will be a constant value, and the chosen convergence criterion is the mean overall difference between consecutive TVAC solutions:

$$\overline{\Delta u_{\mathrm{lim}}} = \mathrm{mean}(u_{\mathrm{lim}_i} - u_{\mathrm{lim}_{i-1}}) \qquad (47)$$

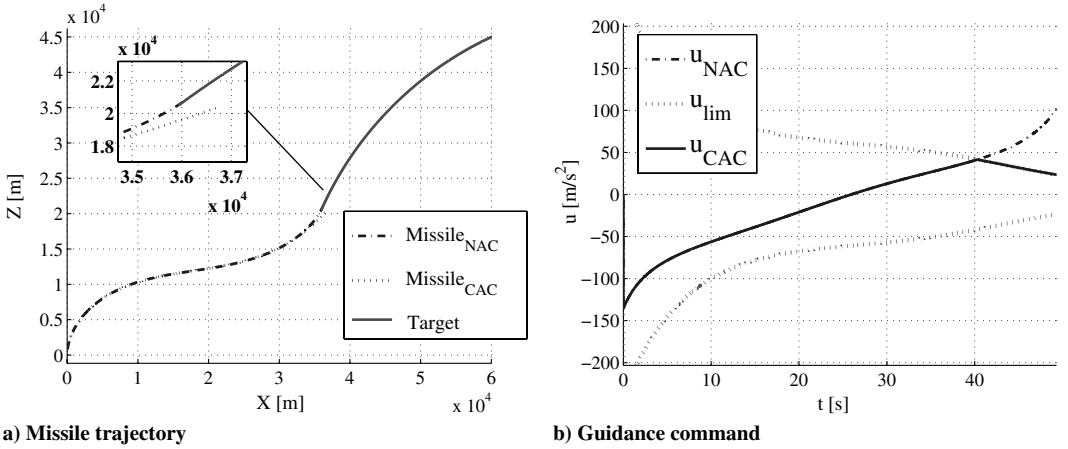

a) Missile trajectory **b) Guidance command**

Fig. 7 Varying acceleration constraint effect on guidance performance.

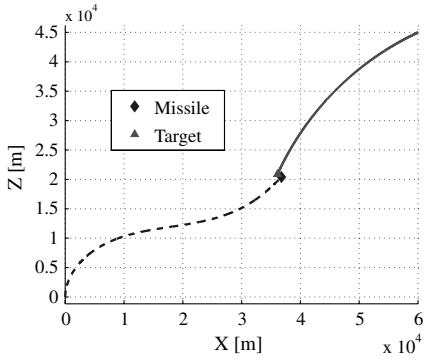

a) Trajectory iteration 1

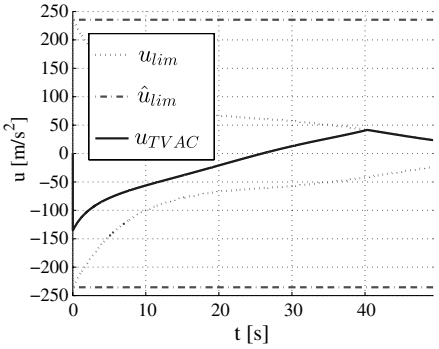

b) Guidance command iteration1

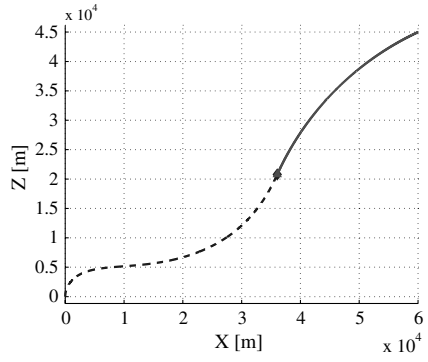

c) Trajectory iteration 2

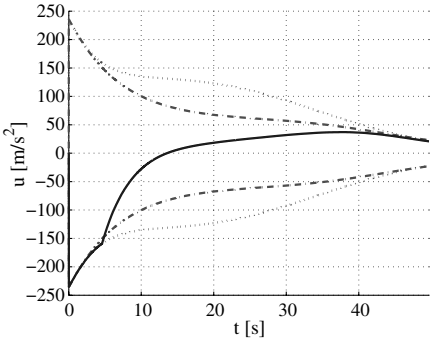

d) Guidance command iteration 2

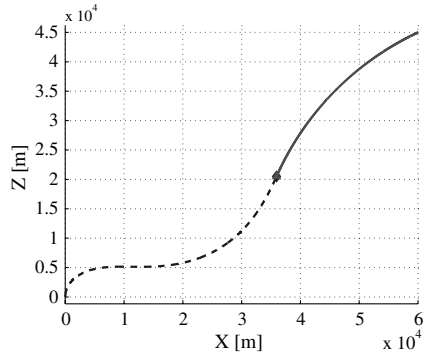

e) Trajectory iteration 3

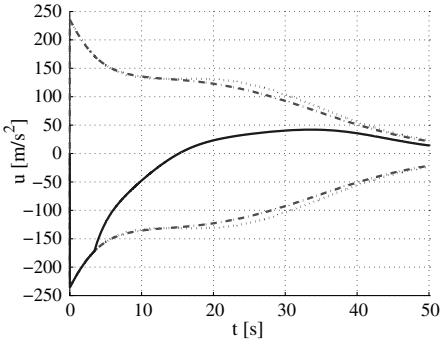

f) Guidance command iteration 3

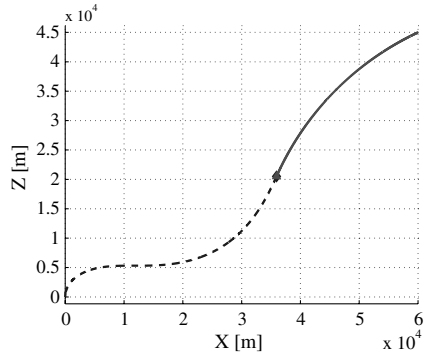

g) Trajectory final

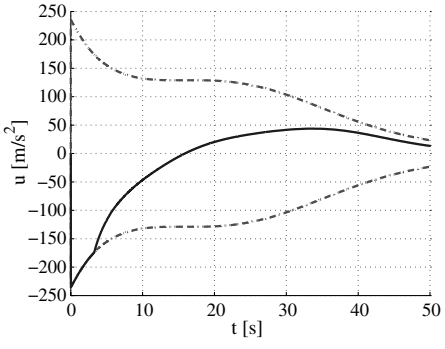

h) Guidance command final

Fig. 8 TVAC iterative computation performed by the guidance algorithm.

The results of the iterative computation procedure are shown in Fig. 8, for the case of a missile with perfect dynamics ($\tau \to 0$). The first step is identical to the CAC case in Sec. VI.B, which is obvious because a CAC has been used as the first guess of the TVAC function. The figure also shows how the TVAC develops from one iteration to another, producing a nearly nonsaturated guidance command along the entire trajectory. The reason a saturation still exists is that u_{lim} was used as a soft constraint rather than a hard one.

D. Time Varying Acceleration Constraint Trajectory Shaping

In an actual engagement, the iterative procedure demonstrated in Sec. VI.C will be calculated once at the beginning of the engagement. Then, the precalculated guidance gains will be used with the guidance command of Eq. (43), and the remaining terms will be estimated in real time. Figure 9a shows the gains obtained by the converged TVAC function. When simulating the actual engagement using these gains, the TVAC trajectory given in Fig. 9b is produced. If the models used in

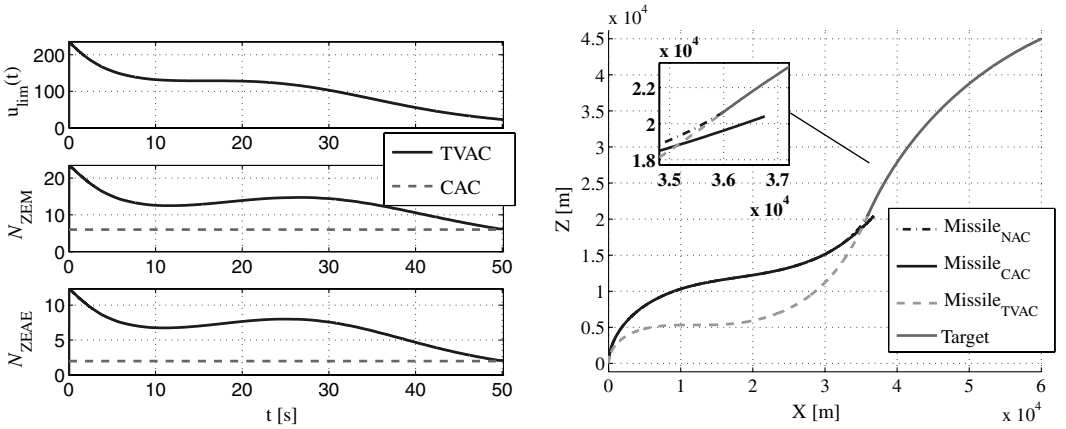

a) TVAC gains final iteration b) TVAC vs. NAC/CAC Trajectories

Fig. 9 TVAC trajectory shaping.

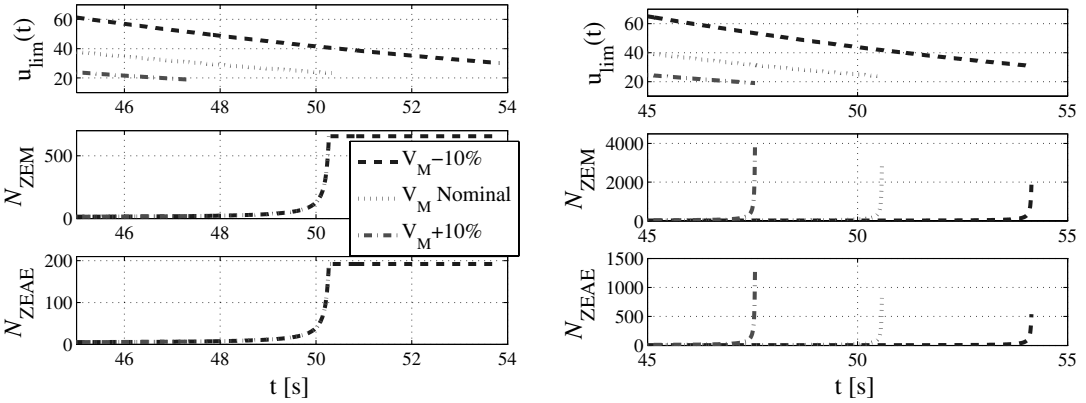

a) TVACD b) TVACND

Fig. 10 TVAC gains dynamic decomposition.

the iterative procedure match the models of the actual engagement, which is the case at hand, the actual trajectory and guidance command will match the last simulated iteration of the TVAC prediction process.

Analyzing Fig. 9a, the gains' initial high values cause the missile to maneuver early in the engagement. Together with Figs. 8h and 9b, it shows how the TVAC optimization shapes the trajectory in a way that keeps the target within the momentary capture region along the entire trajectory; the missile is commanded to bend quicker, obtaining most of the TIAC early and reaching near the collision course, while it is still at a lower altitude and has higher maneuverability.

The fact that the TVAC computation procedure is based on models makes it inherently erroneous; i.e., the atmosphere is a statistical model with considerable variations, the missile's aerodynamics are based on either computational fluid dynamcis and/or wind-tunnel data with a limited accuracy, the target may maneuver differently than expected, etc. If the differences are small enough, and/or if there's enough acceleration margin, a no-capture zone may still be avoided and the proposed guidance law could provide a successful intercept. In cases in which a large error begins to develop between the predicted TVAC and the actual real-time calculated value, the iterative procedure may be repeated online from time to time in order to update the gains history. Between these updates, a real-time feedback command will still be used, using the last updated history.

E. Optimization Decomposition

In this subsection, the contribution of the decomposed optimization for a missile with first-order autopilot dynamics will be examined. Three guidance laws will be compared: u^*_{TVAC}, u^*_{TVACD}, and u_{TVACND}. The TVAC will be computed iteratively as before, though this time a missile with autopilot dynamics will be modeled, and each guidance law will use its own type of gains: u^*_{TVAC}, without dynamics; u^*_{TVACD}, with dynamics; and u_{TVACND}, with normalized dynamics. Then, the simulation will be run again with the predicted gains but with a different missile speed ($\pm 10\%$), simulating variations in the atmosphere, the missile's aerodynamic model, and target speed/maneuver. An autopilot time constant of 1 s will be used, which is relatively large, in order to obtain a noticeable degradation in guidance performance in cases in which the lag is not compensated properly.

It is noted that, although the variation in the actual engagement duration could be addressed by a periodic online update of the u^*_{TVACD} gains (rerunning the iterative procedure at small enough intervals), such an approach might not always be applicable, as it is computationally more demanding and might overload the missile's CPU. Furthermore, as was shown in Sec. IV, the dominant influence near intercept is mostly due to the autopilot lag, whereas the TVAC influence is negligible (the gains converge to CAC). Therefore, this solution would be less efficient at this point.

Referring to Fig. 10a, the gains of u^*_{TVACD} rise too early, both for the nominal[¶] and for the lower-speed cases. The reason for the early rise in the nominal case is that although the solution has converged with a small consecutive error the error still exists, which means that the nominal case may be shorter or longer than the last run of the iterative solution. This error can be reduced with additional iterations, but because computational affordability is required the iterative procedure would be stopped as soon as possible, that is, without compromising the trajectory shaping. The early rise in the lower-speed case was indeed expected, and in this case the gains have reached extremely large values some 4 s before the scenario has ended, which is an undesirable outcome. In the case of the higher speed, the engagement has ended before the final running time of the nominal u^*_{TVACD} solution, and therefore the gains have risen,[**] but not enough and with

[¶]This may not seem clear in the figure due to resolution limitations.

[**]See the preceding footnote.

Table 1 Intercept errors and guidance cost

Speed variation	Miss distance, m/Intercept angle error, deg			$\bar{J} = \frac{1}{t_f}\int_0^{t_f} \frac{u^2}{u_{\lim}^2}\,dt$		
	u^*_{TVAC}	u^*_{TVACD}	u_{TVACND}	u^*_{TVAC}	u^*_{TVACD}	u_{TVACND}
$V_m - 10\%$	0.20/0.11	2.20/ − 0.68	0.01/0.02	3.59E + 00	9.16E + 05	1.41E − 01
$V_m + 0\%$	0.25/0.04	0.05/0.02	0.02/0.02	1.24E + 01	2.29E − 01	2.44E − 01
$V_m + 10\%$	0.02/0.06	6.27/1.13	0.04/0.01	3.78E − 01	1.84E + 04	3.57E − 01

an incorrect timing. As for the decomposed solution u_{TVACND}, shown in Fig. 10b, the gains have risen exactly before intercept with proper timing, in all three cases, because the dynamic effect is timed by the real-time calculated value of t_{go} and not by the predicted one.

Table 1 summarizes performance of the three guidance laws. Looking at the nominal scenario, it is clear that the autopilot dynamics compensation improves the guidance performance (u^*_{TVACD} vs u^*_{TVAC}), as expected, and that u_{TVACND} is suboptimal (a higher cost when compared with u^*_{TVACD}), also as expected. For $V_M \neq V_{M_{\mathrm{Nominal}}}$, the performance of u^*_{TVACD} deteriorates substantially, even worse than u^*_{TVAC}, because of the wrong timing of the increasing of the gains. The performance of u_{TVACND}, on the other hand, remains indifferent to changes in the actual engagement time, as anticipated, thanks to the real-time computation of the CACD gains.

It should also be noted that although u^*_{TVAC} has obtained a smaller miss distance with an increased speed this result is not consistent and strongly depends on the specific state of the system near intercept, the value of the gains, and the autopilot's model. In this specific example, the gains were higher than their CAC values upon intercept because of the TVAC shaping. These smaller intercept errors can be reproduced for any first-order autopilot dynamics, simply by using slightly higher gains. However, this would also increase the guidance cost, and, as previously stated, the results are not consistent and could deteriorate with a slight alteration of the engagement time.

VII. Evaluation of the Time Varying Acceleration Constraint Prediction Method

In Sec. V.A, an iterative method for predicting the TVAC function along the expected trajectory was proposed. When doing so, three immediate questions arise:

1) Is the method computationally affordable?

2) Is the iterative procedure stable; i.e., would it always converge?

3) When the iterative procedure does converge, would it provide the optimal trajectory?

Although this paper will not provide rigorous answers to these questions, it will provide a few observations and insights in the following section.

A. Computational Affordability

The sole purpose of the iterative procedure is to sample the TVAC along the expected trajectory and provide the guidance gains history. Then, the real-time guidance command would use these gains in an open-loop scheduling, in which the intercept errors ($\mathrm{ZEM}/t_{\mathrm{go}}^2$ and $\mathrm{ZEAE}/t_{\mathrm{go}}$) are estimated in real time. In practice, this means that the simulations used in the iterative procedure need not be highly accurate and a relatively large time step can be used, making this procedure potentially quite affordable.

When a fully detailed three-DOF simulation was used, including atmosphere, aerodynamics, thrust, and gravity models, a single iteration that simulated a total intercept time of 85 s, while using a time step of 0.01 s (8500 steps in total), needed approximately 2 ms of CPU time when running on a single core of an Intel® Core2 Duo E8400 processor clocked at 3.00 Mhz.

The example given in Sec. VI.C needed only four iterations in order to converge. In most of the scenarios tested, this procedure needed no more than approximately 5 to 10 iterations, and reaching up to 15 to 20 iterations in extremely marginal cases. This means that the TVAC computation procedure would usually take between 0.4 to 1.65 ms per one simulated second of the engagement. For example, an engagement with a total length of 100 s would require between 40 and 165 ms at most. Considering that the procedure may be used only once at the beginning of the engagement or several times throughout the engagement, periodically with large intervals between updates, the proposed guidance law is indeed affordable.

B. Convergence

The TVAC iterative calculation has been tested on various scenarios with different combinations of initial and final conditions, including different TVAC functions. In most cases, a convergence has been successfully achieved. In fact, it has been very difficult finding cases that do not converge. The few nonconverging cases that were found involved extremely marginal lateral acceleration clearance. An example of such a case is given in Fig. 11, in which two consecutive iterations are presented for a 90 deg intercept angle. The guidance command in this scenario was not limited, but the TVAC trajectory shaping was used. Looking at Fig. 11b, the maximal penalty at the ith iteration, i.e. the ratio $1/u_{\lim}^2$, is reached approximately between 20 and 30 s from the beginning of the engagement. As a result, in the next iteration $(i+1)$ the trajectory was shaped so that the penalty would be lower at that area: the missile was commanded to bend further and remain at lower altitude. This, however, resulted in a higher penalty near intercept, as the intercept occurred at higher altitude where the missile had less maneuverability. This, however, resulted in a higher acceleration demand near intercept, as most of the TIAC had not yet been obtained. This higher demand had exceeded the local acceleration limit, and thus the maximal penalty had shifted to the end of the engagement. The following iterations repeated this pattern, in which the maximal penalty shifted back and forth without converging. If the acceleration clearance were larger just enough in these critical areas, a convergence would have been obtained. However, from a designer's point of view, even if the acceleration clearance were large enough to allow convergence, the missile's operational envelope should not include these scenarios, or the missile should be redesigned to achieve more lift, as it does not leave enough margin to overcome model uncertainties.

C. Optimality of Converged Trajectories

To evaluate the optimality of the converged trajectories, the optimal trajectories of the accurate nonlinear problem must be found first. For this purpose, the General Pseudospectral Optimization Software (GPOPS) is used as a reference. GPOPS is a program written in MATLAB for solving multiple-phase optimal control problems,[††] based on the Radau pseudospectral method. The nonlinear kinematics model used in GPOPS is given by

$$\mathbf{x} = \begin{bmatrix} x_M \\ z_M \\ x_T \\ z_T \\ x_T - x_M \\ z_T - z_M \\ \gamma_M \\ \gamma_T \\ \gamma_I \end{bmatrix}, \qquad \dot{\mathbf{x}} = \begin{cases} \dot{x}_1 = v_M \cos(x_7) \\ \dot{x}_2 = v_M \sin(x_7) \\ \dot{x}_3 = v_T \cos(\pi - x_8) \\ \dot{x}_4 = v_T \sin(\pi - x_8) \\ \dot{x}_5 = \dot{x}_3 - \dot{x}_1 \\ \dot{x}_6 = \dot{x}_4 - \dot{x}_2 \\ \dot{x}_7 = u/v_M \\ \dot{x}_8 = a_T/v_T \\ \dot{x}_9 = \dot{x}_7 + \dot{x}_8 \end{cases} \tag{48}$$

[††]Although optimization programs such as GPOPS are capable of providing the optimal trajectory, much like the solutions in [19,21,24] they need to be continuously run during the engagement in order to provide a feedback-type command, which makes them computationally expensive. In addition, their complexity would require extensive validation.

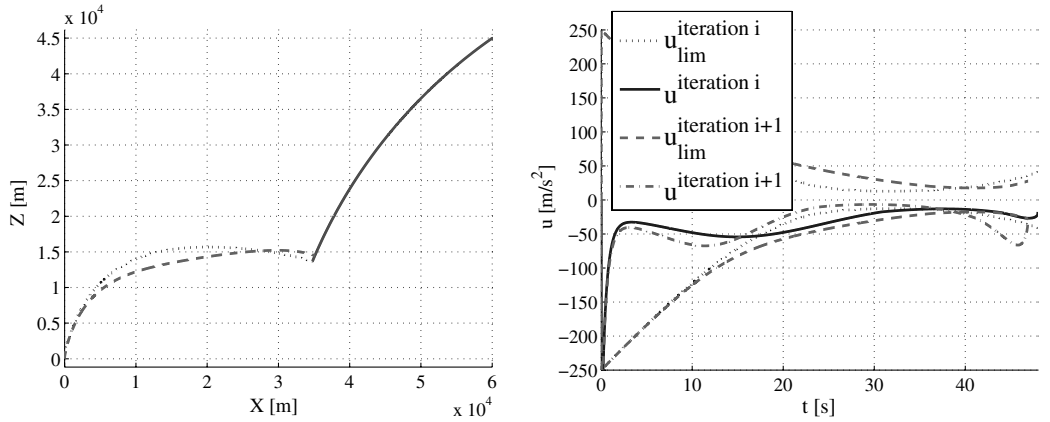

a) Missile trajectory **b) Guidance command**

Fig. 11 Nonconverging example.

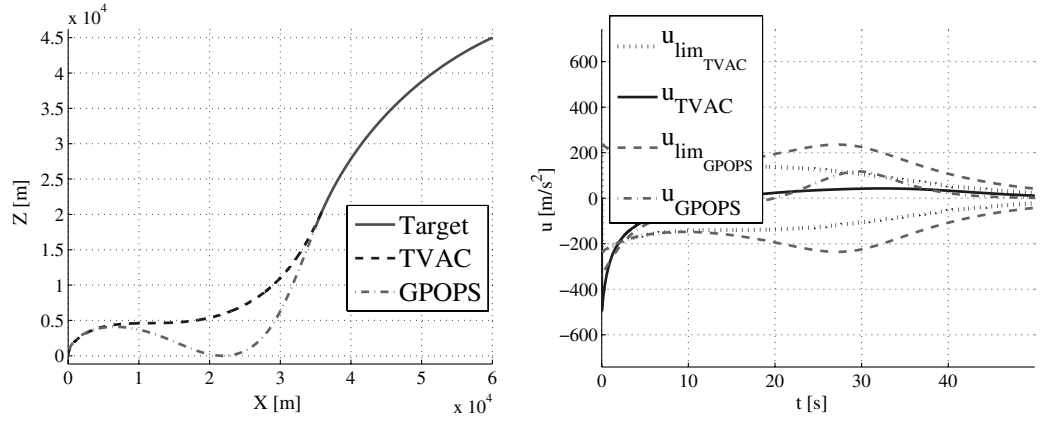

a) Missile trajectory **b) Guidance command**

Fig. 12 TVAC converged trajectory vs GPOPS.

subject to the boundary conditions

$$\mathbf{x}(t_0) = \mathbf{x}_0, \qquad x_5(t_f) = 0, \qquad x_6(t_f) = 0, \qquad x_9(t_f) = \gamma_I^C \tag{49}$$

and the cost function

$$J = \int_0^{t_f} \frac{u^2}{u_{\text{lim}}^2}\,\mathrm{d}t \tag{50}$$

where (x_M, z_M) and x_T, z_T are the missile and target coordinates within the reference frame, respectively.

The Hamiltonian of the nonlinear problem is given by

$$H = \lambda^T \dot{\mathbf{x}} + \frac{1}{2}\frac{u^2}{u_{\text{lim}}^2} \tag{51}$$

and the optimal controller must satisfy

$$H_u = \frac{\lambda_7 + \lambda_9}{V_M} + \frac{u}{u_{\text{lim}}^2} = 0 \tag{52}$$

Figure 12 shows a comparison between TVAC and GPOPS for the example given in Sec. VI.A, in which the missile has perfect dynamics. To obtain a correct comparison, the guidance commands in both simulations were not limited, as the proposed guidance law was obtained without using a hard command constraint. Although not shown in the paper, the minimum principal (i.e., $H_u = 0$) along the GPOPS trajectory has been checked, and it has been confirmed that the trajectory is indeed optimal.

The trajectories are obviously quite different. It is clear from this example that the TVAC converged solution does not necessarily provide the optimal trajectory. This result leads to the following question: does the iterative procedure fail to converge to the optimal trajectory due to the search method used, or is it a result of the linearization around the collision course?

To provide a possible answer, the following test will be performed: the TVAC function will be calculated along the optimal trajectory provided by GPOPS. Then, the gains $N_{\text{ZEM}_{\text{TVAC}}}$ and $N_{\text{ZEAE}_{\text{TVAC}}}$ and the resulting TVAC guidance command u^*_{TVAC} will be calculated along this trajectory. The result of this computation is shown in Fig. 13, compared with the GPOPS command.

The TVAC command is quite different from the optimal command, on the optimal trajectory. The convergence criterion used in the TVAC iterative computation procedure requires that the predicted TVAC would match the actual TVAC along the resulting trajectory. This means that in order to converge to the optimal trajectory the associated TVAC function must reproduce the optimal command. As the preceding example has shown, these two commands are quite different, which explains why the converged and the optimal trajectories are different as well. Two additional questions arise as a result: why are these commands different, and in which cases will they match?

The answer to the first question lies within the linearization; the optimal guidance command was derived under the assumption of the dynamic constraints given in Sec. II.B and the approximation $t_{\text{go}} = -r/V_r$. When the missile and target are far from the collision course, as in the example given, the actual kinematics is not linear, the approximation of t_{go} would be incorrect, and the resulting guidance command will not be optimal. This does not necessarily mean that if the guidance command is not optimal it will not be similar to the

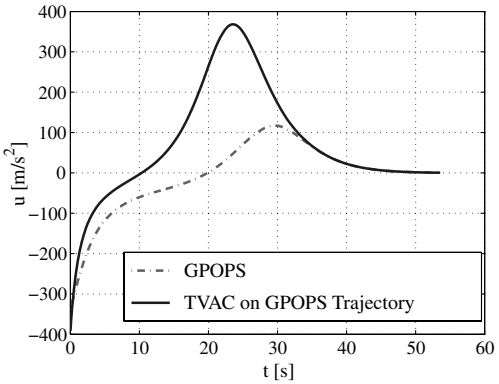

Fig. 13 TVAC guidance command on the optimal trajectory.

optimal command; in some special cases, a nearly optimal command could be reproduced by a combination of erroneous calculations. Studying Fig. 13, the commands seem to match from approximately 35 s (∼25 km downrange), where the missile is near the collision course. In light of this observation, or hint, the second question will be rephrased as follows: if the assumption of linearization is valid on the optimal trajectory, would the TVAC calculation procedure converge to this trajectory?

In an attempt to answer this question, the following simulation tests will be performed for a fixed target, subject to the TVAC function given in Fig. 6:

1) The missile will be positioned on the collision course (zero heading error) while setting the TIAC as the initial LOS angle. Then, the initial heading error will be gradually increased, resulting in larger and larger deviations from the collision course.

2) The test will be repeated, but this time the initial heading error will be set to zero and the TIAC will be gradually increased from the initial LOS angle to different intercept angles.

Because the purpose of the test is to evaluate the TVAC converged trajectories, rather than evaluating the validity of the linearization around the collision course, it is imperative to confirm that substantial trajectory shaping has been made due to the TVAC cost function. For this purpose, these tests will be run for the CAC guidance command as well. The results of these simulative tests are shown in Figs. 14 and 15, in which the missile is initially positioned at the axis origin. Figure 14 shows that the TVAC converged trajectories are very different from the CAC trajectories, confirming that it is the TVAC search method that is evaluated, rather than the validity of the LQ guidance law.

Figure 15 shows that when the optimal trajectory is near the collision course the TVAC search method converges to this trajectory. It also shows that the farther the optimal trajectory is from the collision course the farther the TVAC converged trajectory is from the optimal trajectory. Although this test does not serve as proof, it does give an insight as to how the TVAC converged trajectories are compared with the optimal trajectories.

VIII. Conclusions

In this paper, an optimal control based trajectory shaping guidance scheme has been proposed for a missile with a time varying acceleration constraint (TVAC). The optimization minimizes the ratio between the guidance command and its limit, while still achieving the guidance goal. The time varying guidance gains that allow this trajectory shaping can be calculated easily and relatively quickly, even for complex nonlinear piecewise-continuous acceleration constraints. Because the commands remain of feedback

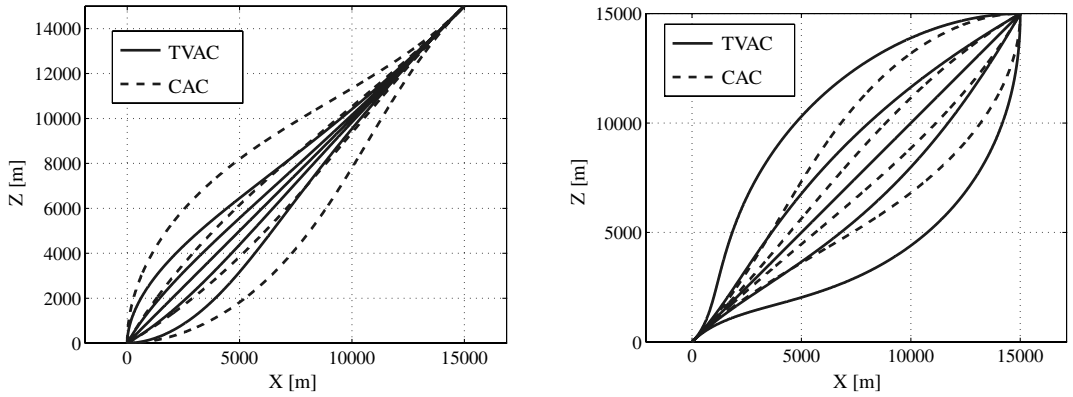

a) Increasing initial heading error **b) Increasing TIAC**

Fig. 14 TVAC converged trajectories vs CAC.

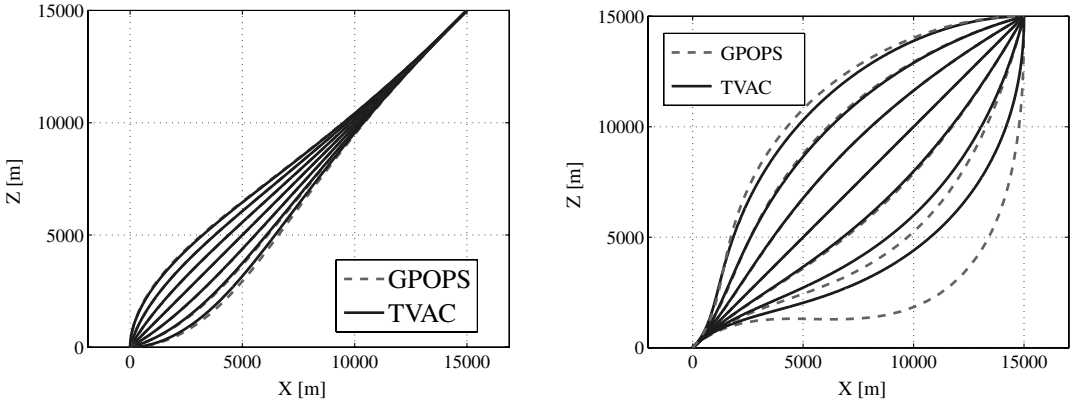

a) Increasing initial heading error **b) Increasing TIAC**

Fig. 15 TVAC converged trajectories vs GPOPS.

type, the guidance scheme remains robust even if the TVAC prediction is somewhat inaccurate or if external disturbances are introduced. The optimization of the guidance command for a missile with autopilot lag has been decomposed to a suboptimal guidance law in order to improve the compensation of the lag under model uncertainties and disturbances. Finally, a comparison with the accurate solution of the nonlinear optimal control problem, supplied with the aid of pseudospectral optimization software, has shown for the different tested scenarios that when the optimal trajectory is near the collision course the guidance scheme proposed in this paper does indeed converge to the optimal trajectory.

Acknowledgment

This research was partially supported by the Israel Science Foundation (grant no. 1423/10).

References

[1] Cho, H., Ryoo, C. K., and Tahk, M. J., "Implementation of Optimal Guidance Laws Using Predicted Missile Velocity Profiles," *Journal of Guidance, Control, and Dynamics*, Vol. 22, No. 4, 1999, pp. 579–588. doi:10.2514/2.4420

[2] Shima, T., and Shinar, J., "Time-Varying Linear Pursuit-Evasion Game Models with Bounded Controls," *Journal of Guidance, Control, and Dynamics*, Vol. 25, No. 3, 2002, pp. 425–432. doi:10.2514/2.4927

[3] Rusnak, I., Weiss, H., Eliav, R., and Shima, T., "Missile Guidance with Constrained Terminal Body Angle," *26th Convention of Electrical and Electronics Engineers*, IEEE Publications, Piscataway, NJ, 2010, pp. 45–49.

[4] Kim, M., and Grider, K. V., "Terminal Guidance for Impact Attitude Angle Constrained Flight Trajectories," *IEEE Transactions on Aerospace and Electronic Systems*, Vol. AES-9, No. 6, 1973, pp. 852–858. doi:10.1109/TAES.1973.309659

[5] Lin, C. F., and Tsai, L. L., "Analytical Solution of Optimal Trajectory-Shaping Guidance," *Journal of Guidance, Control, and Dynamics*, Vol. 10, No. 1, 1987, pp. 61–66. doi:10.2514/3.20181

[6] Kim, B. S., Lee, J. G., Han, H. S., and Park, C. G., "Homing Guidance with Terminal Angular Constraint Against Nonmaneuvering and Maneuvering Targets," *AIAA Guidance, Navigation, and Control Conference*, AIAA, Reston, VA, 1997, pp. 189–199.

[7] Kim, B. S., Lee, J. G., and Han, H. S., "Biased PNG Law for Impact with Angular Constraint," *IEEE Transactions on Aerospace and Electronic Systems*, Vol. 34, No. 1, 1998, pp. 277–288.

[8] Song, T. L., Shin, S. J., and Cho, H., "Impact Angle Control for Planar Engagements," *IEEE Transactions on Aerospace and Electronic Systems*, Vol. 35, No. 4, 1999, pp. 1439–1444. doi:10.1109/7.805460

[9] Zarchan, P., *Tactical and Strategic Missile Guidance*, 4th ed., Vol. 199, Progress in Astronautics and Aeronautics, AIAA, Reston, VA, 2002, pp. 541–569, Chap. 25.

[10] Manchester, I. R., and Savkin, A. V., "Circular Navigation Guidance Law for Precision Missile/Target Engagements," *41st IEEE Conference on Decision and Control*, IEEE Publications, Piscataway, NJ, 2002, pp. 1287–1291. doi:10.1109/CDC.2002.1184692

[11] Ryoo, C. K., Cho, H., and Tahk, M. J., "Closed-Form Solutions of Optimal Guidance with Terminal Impact Angle Constraint," *International Conference of Control Application*, IEEE Publications, Piscataway, NJ, 2003, pp. 504–509. doi:10.1109/CCA.2003.1223469

[12] Ohlmeyer, E. J., "Control of Terminal Engagement Geometry Using Generalized Explicit Guidance," *American Control Conference*, IEEE Publications, Piscataway, NJ, 2003, pp. 396–401. doi:10.1109/ACC.2003.1238981

[13] Lee, Y. I., Ryoo, C. K., and Kim, E., "Optimal Guidance with Constraints on Impact Angle and Terminal Acceleration," *AIAA Guidance, Navigation, and Control Conference*, Austin, TX, CP-5795, AIAA, Washington, DC, Aug. 2003.

[14] Jeong, S. K., Cho, S. J., and Kim, E. G., "Angle Constrained Biased PNG," *5th Asian Control Conference*, IEEE Publications, Piscataway, NJ, 2004, pp. 1849–1853.

[15] Lu, P., Doman, D. B., and Schierman, J. D., "Adpative Terminal Guidance for Hypervelocity Impact in Specified Direction," *Journal of Guidance, Control, and Dynamics*, Vol. 29, No. 2, 2006, pp. 269–278. doi:10.2514/1.14367

[16] Ryoo, C. K., Cho, H., and Tahk, M. J., "Time-to-Go Weighted Optimal Guidance with Impact Angle Constraints," *IEEE Transactions on Control Systems Technology*, Vol. 14, No. 3, 2006, pp. 483–492.

[17] Yoon, M. G., "Relative Circular Navigation Guidance for the Impact Angle Control Problem," *IEEE Transactions on Aerospace and Electronic Systems*, Vol. 44, No. 4, 2007, pp. 1449–1463.

[18] Weimeng, S., and Zhiqiang, Z., "3D Variable Structure Guidance Law Based on Adaptive Model-Following Control with Impact Angular Constraints," *26th Chinese Control Conference*, IEEE Publications, Piscataway, NJ, 2007, pp. 61–66.

[19] Lukacs, J. A., and Yakimenko, O. A., "Trajectory-Shape-Varying Missile Guidance for Interception of Ballistic Missiles During the Boost Phase," AIAA Paper 2007-6538, 2007.

[20] Shima, T., and Golan, O., "Head Pursuit Guidance," *Journal of Guidance, Control, and Dynamics*, Vol. 30, No. 5, 2007, pp. 1437–1444. doi:10.2514/1.27737

[21] Das, P. G., and Padhi, R., "Nonlinear Model Predictive Spread Acceleration Guidance with Impact Angle Constraint for Stationary Targets," IFAC, Seol, Korea, 2008, pp. 13016–13021.

[22] Ratnoo, A., and Ghose, D., "Impact Angle Constrained Interception of Stationary Targets," *Journal of Guidance, Control, and Dynamics*, Vol. 31, No. 6, 2008, pp. 1816–1821. doi:10.2514/1.37864

[23] Shaferman, V., and Shima, T., "Linear Quadratic Guidance Laws for Imposing a Terminal Intercept Angle," *Journal of Guidance, Control, and Dynamics*, Vol. 31, No. 5, 2008, pp. 1400–1412.

[24] Oza, H. B., and Padhi, R., "A Nonlinear Suboptimal Guidance Law with 3D Impact Angle Constraints for Ground Targets," AIAA Paper 2010-8185, 2010.

[25] Shima, T., "Intercept-Angle Guidance," *Journal of Guidance, Control, and Dynamics*, Vol. 34, No. 2, 2011, pp. 484–492.

[26] Ben-Asher, J., and Yaesh, I., *Advances in Missile Guidance Theory*, Progress in Astronautics and Aeronautics, Vol. 180, AIAA, Reston, VA, 1998, pp. 31–69, Chap. 3.

[27] Rusnak, I., and Levi, M., "Modern Guidance Law for High-Order Autopilot," *Journal of Guidance, Control, and Dynamics*, Vol. 14, Sept.–Oct. 1991, pp. 1056–1058.